



Transposable element insertions in fission yeast drive adaptation to environmental stress

Caroline Esnault, Michael Lee, Chloe Ham, et al.

Genome Res. 2019 29: 85-95 originally published online December 12, 2018

Access the most recent version at doi:[10.1101/gr.239699.118](https://doi.org/10.1101/gr.239699.118)

References This article cites 74 articles, 24 of which can be accessed free at:
<http://genome.cshlp.org/content/29/1/85.full.html#ref-list-1>

License This is a work of the US Government.

Email Alerting Service Receive free email alerts when new articles cite this article - sign up in the box at the top right corner of the article or [click here](#).

A promotional banner for CRISPR and RNAi Genetic Screening. The text on the left reads "CRISPR and RNAi Genetic Screening. Your new superpower." To the right is a "LEARN MORE" button. Further right is an image of a woman in a red and white superhero costume with a red mask. To the right of the image is the "CELLECTA" logo, which consists of a cluster of green dots.

To subscribe to *Genome Research* go to:
<https://genome.cshlp.org/subscriptions>

Published by Cold Spring Harbor Laboratory Press

Research

Transposable element insertions in fission yeast drive adaptation to environmental stress

Caroline Esnault, Michael Lee, Chloe Ham, and Henry L. Levin

Section on Eukaryotic Transposable Elements, Division of Molecular and Cellular Biology, Eunice Kennedy Shriver National Institute of Child Health and Human Development, National Institutes of Health, Bethesda, Maryland 20892, USA

Cells are regularly exposed to a range of naturally occurring stress that can restrict growth or cause lethality. In response, cells activate expression networks with hundreds of genes that together increase resistance to common environmental insults. However, stress response networks can be insufficient to ensure survival, which raises the question of whether cells possess genetic programs that can promote adaptation to novel forms of stress. We found transposable element (TE) mobility in *Schizosaccharomyces pombe* was greatly increased when cells were exposed to unusual forms of stress such as heavy metals, caffeine, and the plasticizer phthalate. By subjecting TE-tagged cells to CoCl_2 , we found the TE integration provided the major path to resistance. Groups of insertions that provided resistance were linked to TOR regulation and metal response genes. We extended our study of adaptation by analyzing TE positions in 57 genetically distinct wild strains. The genomic positions of 1048 polymorphic LTRs were strongly associated with a range of stress response genes, indicating TE integration promotes adaptation in natural conditions. These data provide strong support for the idea, first proposed by Barbara McClintock, that TEs provide a system to modify the genome in response to stress.

[Supplemental material is available for this article.]

Cells are regularly challenged by environmental stress, to which rapid and robust responses are critical to their survival. To cope with adverse conditions, cells activate transient programs of transcription that alter expression of hundreds to thousands of genes (Morimoto 1998; Chen et al. 2003; Mahat et al. 2016; Vihervaara et al. 2018). Global response pathways such as those activated by heat shock or hypoxia induce pools of transcriptional *trans*-activators to trigger rapid expression of gene networks.

Specific and prewired transcription responses have evolved due to frequent exposure to a common set of external stresses. However, it is not clear how cells cope when confronted with environmental shock, defined here as novel stresses or conditions that are unusually prolonged or extreme for which existing responses are inadequate to support survival. Adaptation to environmental shock requires genetic alterations that would typically occur in regulatory regions but could also alter coding sequence. These genetic modifications can clearly be achieved through spontaneous mutations. However, preexisting single-nucleotide mutations are randomly distributed, are mostly neutral or detrimental, and, as a result, would not allow survival to abrupt environmental shock if population sizes are limited. One potential solution is the hypothesis that cells possess a mechanism that responds to environmental changes by increasing errors in DNA replication (Cairns et al. 1988; Cairns and Foster 1991). However, this possibility remains unresolved because model reporters suggest stress-induced growth limitation may not influence replication errors (Roth et al. 2006; Maisnier-Patin and Roth 2015; Yamayoshi et al. 2018). Thus, while point mutations in regulatory or coding sequences have the potential to allow survival following environmental shock, they may often be inadequate.

Transposable elements (TEs) are genetically diverse mobile sequences that have proliferated extensively throughout eukaryotic

genomes. These mobile elements respond to stress and through integration alter genome structure (Horvath et al. 2017). In her seminal studies of maize, Barbara McClintock discovered TEs and found their mobility allows them to “enter and take over control of genes” (McClintock 1984). We now know that TEs carry regulatory elements that can control genes by altering their transcription and splicing (Jordan et al. 2003; Bourque et al. 2008; Faulkner et al. 2009). The high copy numbers of TEs, together with their regulatory sequences, cause them to have a large role in shaping the transcriptome. TE sequences are estimated to be present in 25% of human promoters (Jordan et al. 2003), and genome-wide studies of transcription demonstrate that TEs provide a substantial fraction of tissue-specific and alternative promoters (Faulkner et al. 2009; Macfarlan et al. 2012; Mele et al. 2015). This ability of TEs to impact transcription adds support to McClintock’s proposal that TEs provide a means to overcome the threat of environmental shock by reorganizing the genome (McClintock 1984). Despite many reports that TEs are induced by stress and despite examples of individual integration events that result in growth phenotypes, the tenet that TE mobility provides a program that overcomes environmental stress has not been directly tested.

TEs of model organisms provide a unique opportunity to study the biological impact of active transposition in genetically tractable systems (Curcio et al. 2015; Eickbush and Eickbush 2015; Esnault and Levin 2015; Majumdar and Rio 2015; Sandmeyer et al. 2015; Sultana et al. 2017). Integration of the LTR retrotransposon Tf1 of *Schizosaccharomyces pombe* has been studied by determining as many as 1 million integration events with high-throughput sequencing (Guo and Levin 2010; Chatterjee et al. 2014; Esnault and Levin 2015; Hickey et al. 2015). The overwhelming majority of *de novo* insertions cluster in the nucleosome-depleted region of RNA polymerase Pol II-transcribed promoters. Importantly, the insertions are directed to approximately 1000 promoters with an enrichment for stress

Corresponding author: henry_levin@nih.gov

Article published online before print. Article, supplemental material, and publication date are at <http://www.genome.org/cgi/doi/10.1101/gr.239699.118>.

This is a work of the US Government.

response genes (Guo and Levin 2010; Chatterjee et al. 2014). This highly selective integration pattern is mediated by Sap1, a factor that interacts with Tf1 integrase and binds selectively to the promoters at the precise positions where insertions occur (Hickey et al. 2015; Jacobs et al. 2015). A stress response enhancer imbedded in Tf1 causes integration to induce the expression of adjacent promoters (Leem et al. 2008; Feng et al. 2013). The prominent clustering of integration in promoters and the influence of the Tf1 enhancer on adjacent genes suggest the intriguing possibility that Tf1 may be wired to provide a genetic system for efficient adaptation to environmental stress.

Results

Diverse forms of stress activate transcription and retrotransposition

The expression of many TEs is induced by stress conditions (McClintock 1984; Chen et al. 2003; Hashida et al. 2003; Todeschini et al. 2005; Hashida et al. 2006; Sehgal et al. 2007; Chénais et al. 2012; Jardim et al. 2015; Miousse et al. 2015; Morales et al. 2015). This includes single-copy Tf1 elements previously shown to be induced by heat shock and oxidative stress (Feng et al. 2013). We explored the possibility that Tf1 responds to environmental shock by measuring its expression in cells subjected to the heavy metal CoCl_2 (Fig. 1A). Of four single-copy Tf1 elements previously found to be induced by heat shock, CoCl_2 significantly increased expression of three out of four (Fig. 1B; Feng et al. 2013).

Although stress-induced transcription of many TEs can be readily documented, it is difficult to determine whether this expression results in increased transposition events. We were able to measure transposition rates of the same four single-copy Tf1 elements using an assay that relies on a *neo* gene disrupted with an artificial intron (AI) (Atwood et al. 1998; Rai et al. 2017). We found three of the four single-copy Tf1 elements generated six- to 139-fold higher rates of transposition when cells were exposed to CoCl_2 for 24 h (Fig. 1C). We further explored the biological importance of activated transposition by exposing cells to a range of unusual stress conditions. Indeed, transposition of these single-copy Tf1 elements was induced by growing cells in another heavy metal, ZnCl_2 (Fig. 1C). Importantly, transposition was also stimulated by agents foreign to *S. pombe* such as caffeine and a ubiquitous environmental pollutant, the plasticizer phthalate (Fig. 1C). Interestingly, no correlation was observed between rates of transposition and growth rates on media containing the stress agents (Supplemental Fig. S1). Transposition induced by such a range of unusual stress conditions indicates that Tf1 may stimulate adaptation of *S. pombe* to environmental shock.

Competition in CoCl_2 identifies groups of insertions that improve resistance

Although the distribution of insertions to stress promoters (Guo and Levin 2010; Chatterjee et al. 2014; Esnault and Levin 2015; Hickey et al. 2015) and the activation of adjacent genes (Feng et al. 2013) suggest Tf1 has the means to increase resistance to stress, there are other scenarios. To test whether transposition does play a significant role in adaptation, we conducted controlled experiments with laboratory strains. We challenged populations of highly characterized laboratory isolates by passaging them in medium containing different concentrations of a broad range tox-

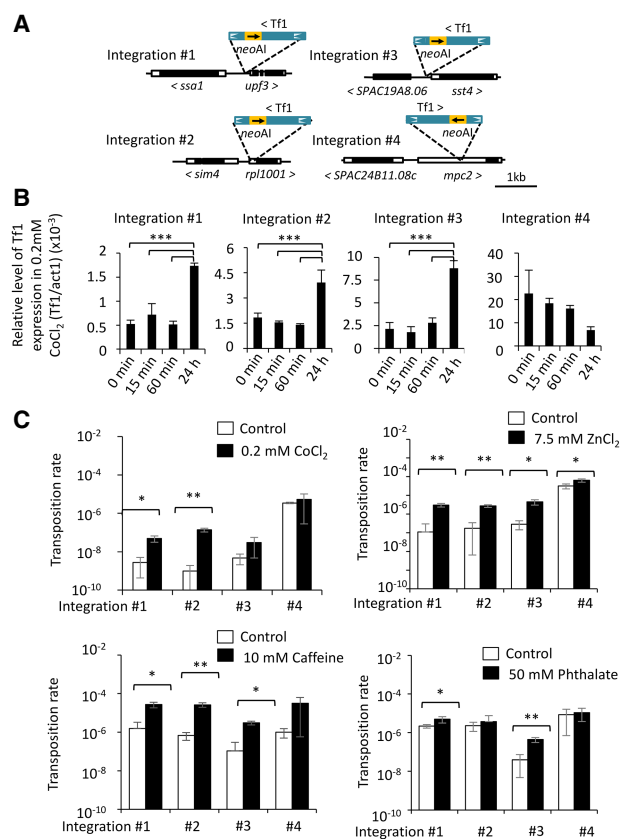


Figure 1. Diverse forms of environmental stress induce Tf1 expression and transposition. (A) Tf1 integration sites generated in a previous study (Feng et al. 2013). For mobility assays, we added an artificial intron in *neo* (*neoAI*). White boxes indicate UTR; black boxes, ORF; line, intergenic region. (B) Relative level of Tf1 mRNA over time during exposure to CoCl_2 . (C) Tf1 transposition rate after exposure to CoCl_2 , ZnCl_2 , caffeine, and phthalate. Differences that are significant are indicated as follows: (*) $P \leq 0.05$; (**) $P \leq 0.005$; (***) $P \leq 0.0005$.

in that is not common in natural substrates. We selected CoCl_2 in part because it generates reactive oxygen species, causes DNA damage, induces apoptosis, and mimics hypoxia (Lee et al. 2007; Simonsen et al. 2012; Gallo et al. 2014; Zhong et al. 2014, 2015; Yang et al. 2015; Tan and Miyamoto 2016). Unlike the experiments in Figure 1 where CoCl_2 stimulated rates of de novo integration of 1×10^{-7} per cell per generation, here we used cultures where each cell contained one of 41,000 preestablished insertions of Tf1-*neo* that we created by overexpression of Tf1 followed by selection for integration events (Methods; Supplemental Fig. S2). Each cell contained a specific insertion that served as a tag that we used to measure clonal expansion during competitive growth. With high-throughput sequencing of the Tf1-*neo* tags, we monitored clonal expansion in cultures grown for 80 generations in 0.0, 0.2, or 1.2 mM CoCl_2 (Fig. 2A). Three independent passaging experiments were conducted for each CoCl_2 concentration. The 0.2 mM CoCl_2 caused modest reductions in growth in each passage, while 1.2 mM CoCl_2 resulted in greater impairment, particularly during passage no. 2 (Fig. 2B).

We monitored changes in the populations of clones in the final cultures ($T = 80$) relative to their prominence in the initial culture ($T = 0$). Spontaneous mutations that improve growth would lead to significant increases in the integration tag present in the

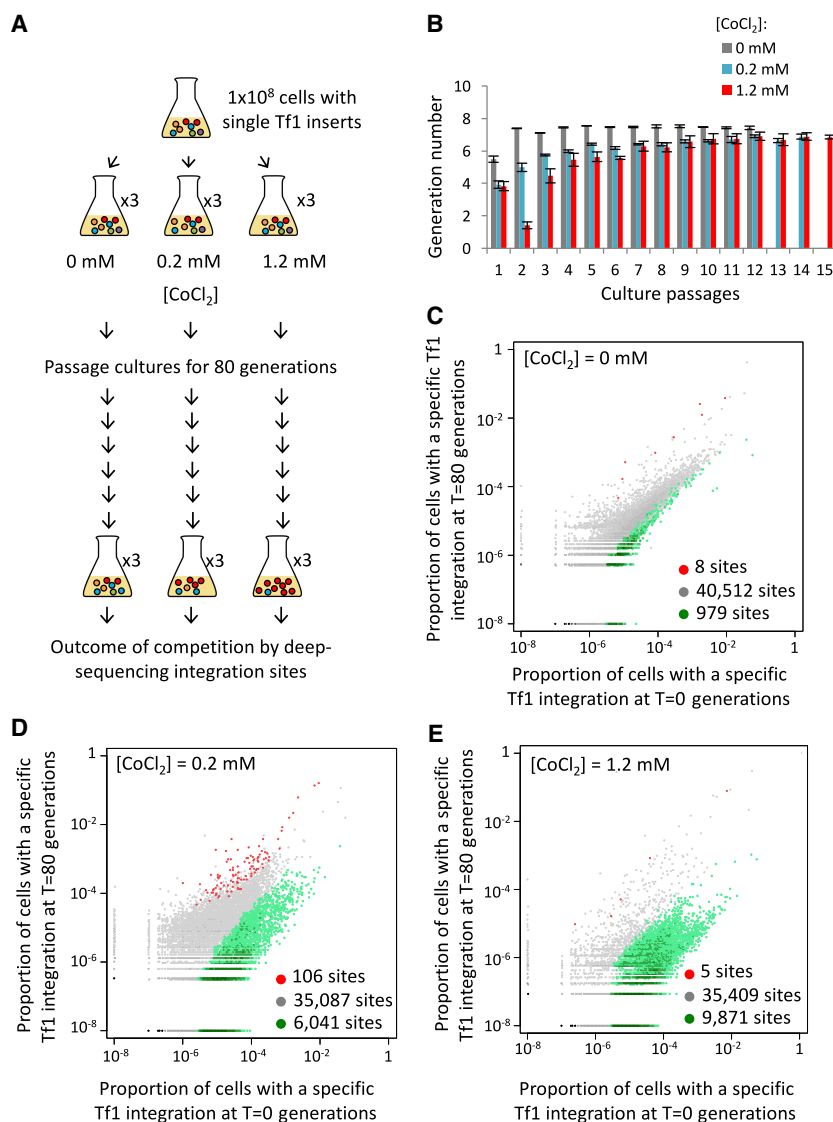


Figure 2. A reproducible set of Tf1 integration tags showed improved growth in CoCl₂. (A) Cells with Tf1 integration tags were passaged for 80 generations in CoCl₂. Changes in clonal populations were monitored by sequencing the tags at $T=0$ and $T=80$ generations. (B) Number of generations observed per 24-h passage. (C–E) Proportions of cells in the cultures containing a Tf1 integration tag at each of the insertion sites at the beginning ($T=0$; x-axis) versus the end ($T=80$; y-axis) of the passages without CoCl₂ (C) or in the presence of 0.2 mM (D) or 1.2 mM (E) CoCl₂. Insertion site tags that changed twofold or more in all three replicated experiments are considered to have expanded (red) or diminished (green).

mutated cell, while the same tag would be unlinked to the spontaneous mutation in other independent passaging experiments and would not be expected to increase. We assessed the occurrence of this type of mutation and found no evidence that after 80 generations the passaging experiments were dominated by tags that were exclusive to single experiments.

We next assessed whether the Tf1 insertions themselves provided a prominent path to improved growth by identifying clones that expanded in each of the three independent passaging experiments. If after 80 generations an individual insertion site increased twofold or more in proportion in all three replicated experiments, we considered that site to have expanded (Fig. 2C–E, red), while we considered a site that decreased twofold or more in all replicated experiments to have diminished (Fig. 2C–E,

green). In cultures grown without CoCl₂, the bulk of the insertions (97.6%), (Table 1) did not change in proportion after 80 generations of growth (Fig. 2C, gray; Supplemental Table S1). When these positions were plotted based on their average proportion at $T=0$ versus $T=80$, they fell largely on the diagonal, indicating Tf1 did not significantly impact growth in the absence of CoCl₂ (Fig. 1C).

Much larger changes occurred in the cultures that contained CoCl₂. With 0.2 mM CoCl₂, 106 integration positions reproducibly increased in proportion after 80 generations (Fig. 2D, red; Table 1). That the three sets of enriched positions contained an overlap of 106 sites was highly significant with a hypergeometric $P < 1.47 \times 10^{-44}$. These positions accounted for 3.1% of the initial culture and expanded strikingly to become 58%, 52%, and 31% (average of 47%) of the final cultures for passaging experiments 1, 2, and 3, respectively. These substantial percentages of reproducible tags indicate that the Tf1 insertions contributed significantly to improved growth. There were 6041 positions that decreased twofold or more, accounting for 59.3% of the culture at $T=0$, and that were reduced to 4.0% in $T=80$ (Table 1). In the cultures grown in 1.2 mM CoCl₂, just five integration positions increased twofold or more in the three independent cultures (Fig. 2E, red; Table 1). Growth during the second passage of the 1.2 mM CoCl₂ cultures was greatly restricted, suggesting there was a severe bottleneck that may have limited the diversity of insertions that were beneficial. As a result, the enriched sites differed from culture to culture. A total of 51 integration positions expanded twofold or more in at least one of the independent passaging experiments containing 1.2 mM CoCl₂. As expected for growth in the higher concentration of CoCl₂, more integration

positions decreased in the cultures that contained 1.2 mM CoCl₂ versus 0.2 mM CoCl₂ (Fig. 2E, green).

By analyzing insertion clones in the individual 0.2 mM CoCl₂ passaging experiments, we found a reproducible set of 106 competition-enriched insertions marked the cells with the greatest increase, indicating that the Tf1 insertions themselves contributed the most to improved growth. Sixteen of the 51 positions expanded in 1.2 mM CoCl₂ were also identified in the three replica cultures grown in 0.2 mM, suggesting these sites also improved growth. The increased representation of insertion sites in cells grown in CoCl₂ suggested the possibility that Tf1 improved cell growth by modulating the expression of specific groups of genes. To determine whether specific pathways were implicated, we analyzed the 141 (0.2 mM + 1.2 mM) enriched Tf1 positions

Table 1. Proportion of clonal populations that changed in three independent passaging experiments

Cobalt concentration		0 mM	0.2 mM	1.2 mM
No change	No. of positions	40,512 (97.6%)	35,087 (85.1%)	31,622 (76.2%)
	Proportion of culture at T0	83.7%	37.6%	14.1%
	Proportion of culture at T80	90.6%	49.0%	90.5%
Increase ^a	No. of positions	8 (0.019%)	106 (0.26%)	5 (0.012%)
	Proportion of culture at T0	1.3%	3.1%	0.7%
	Proportion of culture at T80	8.3%	47.0%	7.9%
Decrease ^a	No. of positions	979 (2.3%)	6041 (14.6%)	9871 (23.8%)
	Proportion of culture at T0	15.0%	59.3%	85.2%
	Proportion of culture at T80	1.1%	4.0%	1.6%
Total no. of positions		41,499	41,234	41,498

^aClones of cells tagged with Tf1 integrations were classified as either increasing or decreasing if they changed in proportion twofold or more in all three biological replicates.

and found all but six were in intergenic regions. Two hundred fifty genes adjacent to enriched Tf1 positions in intergenic sequences were evaluated for Gene Ontology (GO) enrichment (Fig. 3A). We found five function, process, and phenotype ontologies were enriched among our gene set (Supplemental Table S2). Ontologies enriched with *P*-values <0.05 included three networks of coregulated genes: Cd-induced, H₂O₂-induced, and Tor1-regulated genes. Altering expression of genes induced by the heavy metal Cd and the oxidizing agent H₂O₂ has the potential to improve growth in CoCl₂. Other processes with *P*-values <0.05 were the 11.6- and 4.9-fold enrichments associated with resistance to canavanine and amino acid import, respectively. It is striking that three groups of significantly enriched genes are associated with the target of rapamycin (TOR) pathways. Amino acid transporters are regulators of the TOR pathways (Chantranupong et al. 2015, 2016; Wang et al. 2015b; Eltschinger and Loewith 2016; Goberdhan et al. 2016; Saxton et al. 2016), and because canavanine is a toxic analog of L-arginine, the resistance mutations are involved in arginine transport (Rosenthal 1977). The enrichment of factors involved in arginine transport is particularly relevant because arginine is a key regulator of TOR (Chantranupong et al. 2015; Rebsamen et al. 2015; Wang et al. 2015b). This association of enriched groups involved in TOR regulation is notable and consistent with the possibility that TOR activity reduces CoCl₂ toxicity.

TOR pathways provide resistance to CoCl₂

TOR pathways rely on highly conserved serine/threonine kinases that control proliferation, survival of environmental stress, and protein translation (Loewith and Hall 2011; Workman et al. 2014; Chantranupong et al. 2015; Weisman 2016). Two evolutionarily conserved TOR complexes (TORC1 and TORC2) participate in pathways that regulate separate and sometimes overlapping processes. The TORC1 complex plays a primary role in regulating growth, while TORC2 is required to survive starvation and a variety of other environmental stresses. In *S. pombe* the nomenclature is awkward as Tor2 is the kinase of the TORC1 complex and Tor1 assembles in the TORC2 complex.

Thirty-six of the genes adjacent to the competition-enriched positions participate in TOR signaling, are involved in amino acid transport, or are regulated by TORC1 (Fig. 3B, blue text). Genes in these groups include Mip1, a core subunit of TORC1; Gtr2 and Vma10, inducers of TORC1; and two key inhibitors of TORC1, Tsc1 and Npr2. Importantly, *sat1*, a direct inducer of TORC2, was also adjacent to an enriched insertion.

We tested whether the TORC1 and TORC2 pathways mitigate cobalt toxicity by growing strains lacking TOR factors on solid media containing a high concentration of CoCl₂. Although wild-type cells grew slowly on plates with CoCl₂, greater defects were observed for strains lacking Tco89 and Tor1, key subunits of TORC1 and TORC2, respectively (Fig. 3C). It was equally significant that strains lacking inhibitors of TORC1 (Tsc1, Tsc2, and Npr2) showed improved growth on CoCl₂. Lack of Sat1, the TORC2 activator, greatly increased sensitivity to CoCl₂. The absence of Sin1, a component of TORC2, also resulted in sensitivity to CoCl₂. These results demonstrate that both TORC1 and TORC2 activity provide resistance to CoCl₂.

Single Tf1 insertions are sufficient for resistance to CoCl₂

The contribution of the TOR pathways to CoCl₂ resistance argues that the Tf1 insertions improved growth by modifying the expression of TOR factors. However, it is possible that the enriched insertions detected are simply passenger mutations and make no direct contribution to CoCl₂ resistance. In addition, the enriched insertions might function in combination with second site mutations to create resistance. Although the reproducibility of the enriched positions indicated the Tf1 insertions play a key role in resistance to CoCl₂ we decided to test directly whether single Tf1 insertions were sufficient to improve growth in CoCl₂.

We tested the contribution of a cadmium-induced gene by recreating a strain with Tf1-*neo* inserted next to *zrt1* at the same nucleotide position and orientation that was enriched in the competition experiments (Fig. 4A, integration 5). We also tested the contribution of modified TORC1 and TORC2 activity by recreating the insertions adjacent to *tsc1* and *sat1*, again at the same nucleotide position and orientation that expanded in the competition cultures (Fig. 4A, integrations 6 and 7). To evaluate their fitness, each of the recreated insertions was combined with equal proportions of cells lacking the insertion and grown in competition for 80 generations. Three independent passaging experiments were performed for each of the reconstructed strains. Surprisingly, wild-type cells lacking the insertions outcompeted each of the three insertions when grown without CoCl₂ (Fig. 4B, left). These results demonstrate that the insertions imposed an overall burden on growth. Importantly, in competition cultures containing CoCl₂, all three insertions significantly outcompeted the wild-type cells lacking the insertions (Fig. 4B, right). This demonstrates these Tf1-*neo* integrations were sufficient to improve growth in CoCl₂.

We next tested whether the inserts altered expression of their adjacent genes. Integration 5 occurred within the 5' UTR of *zrt1*

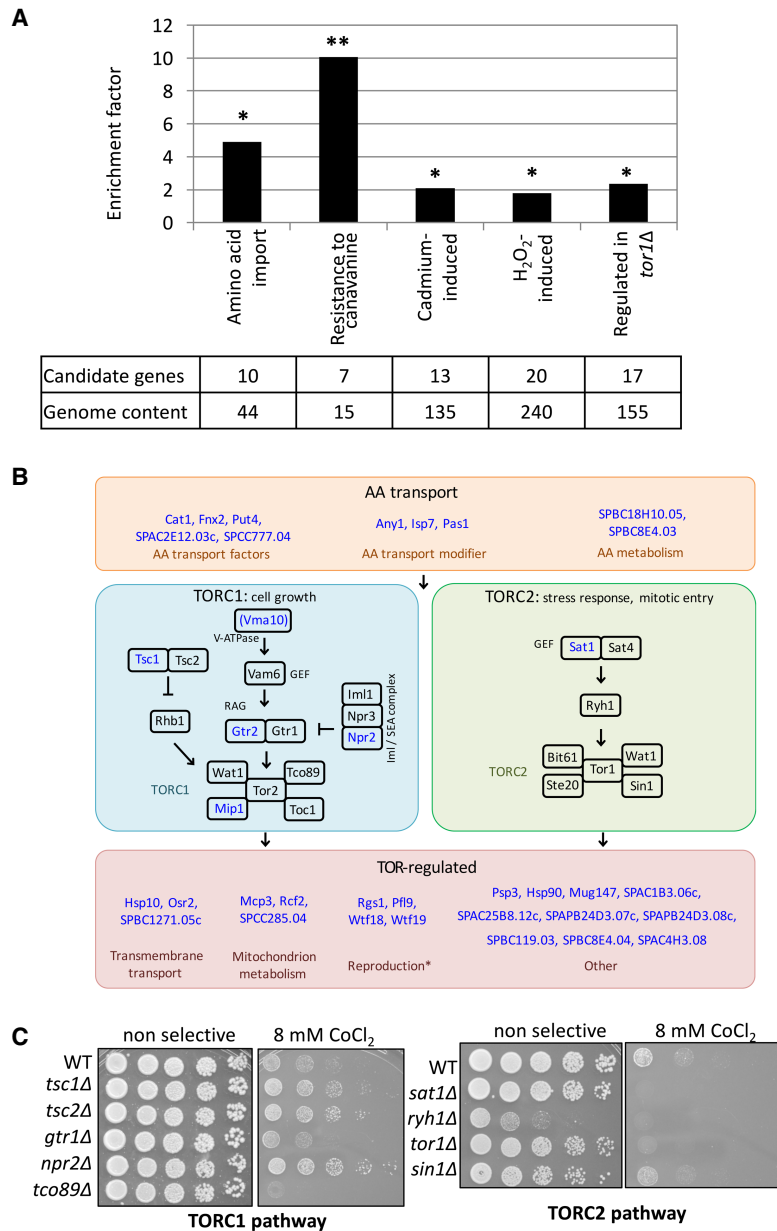


Figure 3. TOR pathways provide resistance to CoCl₂. (A) Ontology of genes adjacent to competition-enriched Tf1 insertions are associated with TOR signaling, stress response, and cation transport. *P*-values based on hypergeometric tests were corrected per gene set by false-discovery rate. (*) *P* ≤ 0.05; (**) *P* ≤ 0.005. (B) Regulatory relationships of genes in the TOR pathways. Intracellular amino acid concentrations regulate TORC1 and TORC2, leading to the regulation of various downstream processes. Thirty-six genes shown in blue were adjacent to competition-enriched Tf1 insertion tags. Reproduction* indicates genes involved in mating and meiosis. (C) Growth phenotype on solid media containing CoCl₂ of cells lacking factors in TORC1 and TORC2 pathways.

69 bp downstream from the start of transcription. RT-qPCR analysis of RNA from cultures showed that this Tf1 insert profoundly reduced *zrt1* mRNA regardless of whether CoCl₂ was present (Fig. 4C). This insertion had no effect on the expression of the other flanking gene, *mok13* (located 2.3 kb upstream). These results indicate that the improved growth in CoCl₂ caused by integration 5 was likely due to reduced expression of *zrt1*.

Integration 6 was inserted 130 bp upstream of the 5' UTR of *tsc1* and 625 bp upstream of the 5' UTR of *rgs1*. This insertion signif-

icantly reduced both *tsc1* and *rgs1* mRNA in cultures lacking CoCl₂. However, in the presence of CoCl₂, only the expression of *tsc1* was reduced, indicating that the lower levels of *tsc1* expression likely caused the improved growth in the competition experiments (Fig. 4C).

Integration 7 was positioned in the 3' UTR of *sat1* 193 bp after the stop codon and 3.8 kb upstream of the *ssn6* 5' UTR. This insertion caused increases in *sat1* mRNA especially in the presence of CoCl₂, whereas no change in *ssn6* mRNA was observed (Fig. 4C). It is therefore likely that integration 7 improved growth in CoCl₂ by increasing TOR activity or reducing amounts of a key metal uptake factor, *Zrt1* (Dainty et al. 2008).

In wild isolates of *S. pombe*, LTRs are enriched in promoters of stress response genes

If transposition makes an important contribution to adaptation, we expect that in wild isolates of *S. pombe*, insertions would be associated with genes known to mitigate stress. We explored this possibility by examining the genomic positions of 1048 LTRs from 57 genetically distinct wild strains of *S. pombe* isolated from around the globe (Jefferes et al. 2015). These LTRs clustered in promoter sequences similar to what is observed for de novo integration of Tf1 (Supplemental Fig. S3; Guo and Levin 2010; Chatterjee et al. 2014; Esnault and Levin 2015; Hickey et al. 2015). We evaluated the potential impact of recent integration events on adaptation to stress by analyzing the 859 LTRs that are polymorphic among the collection of wild strains. Ontology screens of the genes flanking the LTRs revealed high enrichment of activity that contributes to sporulation frequency in many of the wild isolates (Fig. 5A). These enrichments occurred in multiple yeast clades, indicating the clusters of LTRs adjacent to sporulation efficiency genes

formed independently in different populations (Fig. 5B). The reoccurring clusters of LTRs at sporulation frequency genes are consistent with the independent adaptation that would be expected to enhance survival of strains challenged by environmental stress. Genes adjacent to polymorphic LTRs were also enriched with other survival functions such as resistance to heat shock, sensitivity to high osmolarity, and induction by peroxide (Supplemental Fig. S4). A formal possibility was that these promoters were under reduced purifying selection, which would account for their observed

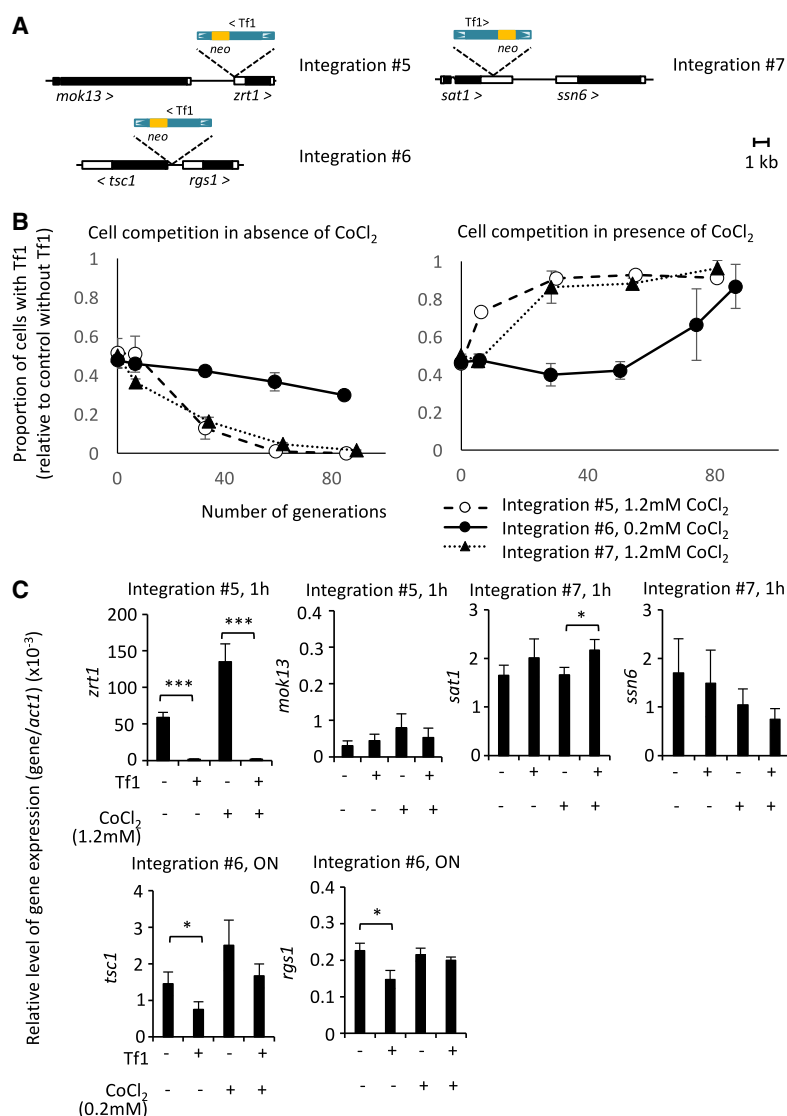


Figure 4. Single Tf1 insertions were sufficient for resistance to CoCl₂ by regulating expression of adjacent genes. (A) The genomic context of enriched Tf1 integration tags reconstructed by homologous recombination. (B) Competition in 0.0 mM (left), 0.2 or 1.2 mM (right) CoCl₂ between cells lacking Tf1 and cells containing genomic integrations 5, 6, or 7. (C) Relative level of expression of genes adjacent to Tf1 integration sites. (ON) Overnight exposure to stress.

enrichment of LTRs. However, a test that uses single-nucleotide polymorphisms (Tajima's *D*) (Tajima 1989) found selection in regions adjacent to stress and sporulation frequency genes was similar to the regions adjacent to genes used as background. The enrichment of polymorphic LTRs adjacent to genes involved in sporulation and stress conditions indicates that retrotransposition in *S. pombe* could promote survival in wild conditions. The insertion of these LTRs may have been induced by stress conditions since the associated genes respond to the same stresses that in laboratory strains activate Tf1 and the closely related element Tf2 (Chen et al. 2003; Feng et al. 2013).

Discussion

Ever since Barbara McClintock discovered transposable ("controlling") elements in maize, it was appreciated that they are activated

by changes in environmental conditions (Levin and Moran 2011; Horvath et al. 2017). Although increased mobility has long been thought to benefit the host, the precise impact and importance of this activity have not been directly studied.

In asking how cells adapt to stress, we found that TE integration into specific groups of promoters can provide a major path to resistance. The enrichment of LTRs in the stress response promoters of wild isolates of *S. pombe* is evidence that TEs do promote adaptation in natural conditions. Our TE tagging of strains with individual insertions allowed us to quantify the fraction of cells that gained resistance to CoCl₂ in independent passaging experiments. While the 106 competition enriched positions represented 3.1% of the starting culture, 80 generations of growth in 0.2 mM CoCl₂ caused the enriched positions to comprise 58.1%, 51.5%, and 31.2% of the three passaged cultures. In addition to the substantial resistance provided by integration, it is noteworthy that the fraction of TE-mutated cells that provide resistance (3.1% at T0) actually represented a surprisingly large proportion of all the TE generated mutations. Together, these results indicate that the integration activity of Tf1 provides substantial benefit when cells are subjected to stress.

The high impact of the Tf1 insertions is due in part to the targeting mechanism that directs integration to promoters (Guo and Levin 2010; Hickey et al. 2015) and due to the fact that Tf1 carries an enhancer that increases expression of adjacent genes (Feng et al. 2013). Another key feature of Tf1 function that increases its contribution to adaptation is a bias in the integration mechanism that targets promoters. While insertions occur broadly among about 20% of promoters, they are enriched for promoters induced by the core stress response (Chen et al. 2003), which includes conditions such as heavy metal (Cd), reactive oxygen, heat, DNA damage (MMS), and osmotic stress (Guo and Levin 2010; Chatterjee et al. 2014). A critical feature of Tf1 activity and that of the closely related Tf2 is that their promoters participate in the core stress response showing significant activation when cells are exposed to these stresses (Chen et al. 2003; Feng et al. 2013). Significantly, the activation of Tf1 transcription results in increased integration frequencies (Fig. 1C). As a result, each of these features, increased mobility, targeting of promoters, and the stimulation of adjacent genes, promotes adaptation. Having observed these properties, we propose that Tf1 is a highly evolved mutagenic system that benefits the host by driving adaptation to environmental insults (Fig. 6).

The activation of Tf1 mobility is observed in a surprising diversity of stress conditions, including CoCl₂, caffeine, and

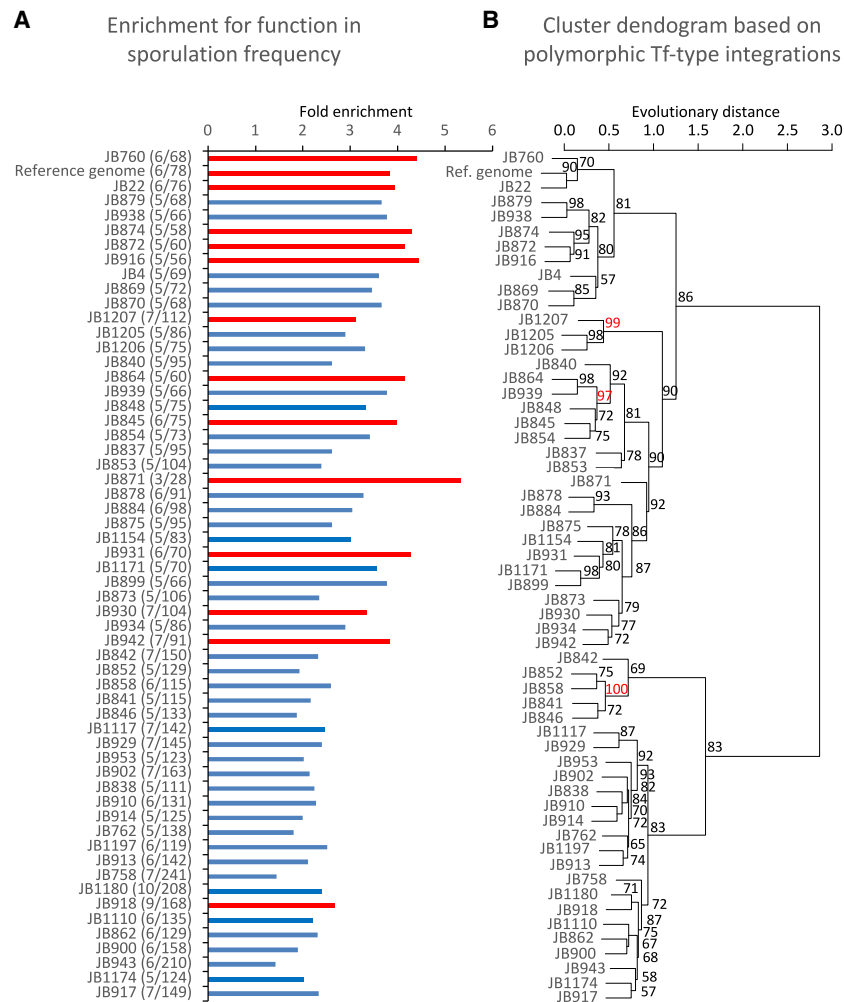


Figure 5. Polymorphic Tf insertions found in wild strains clustered next to sporulation frequency genes. (A) Enrichment for the term “decreased sporulation frequency” for genes adjacent to polymorphic LTRs in wild strains. The number of sporulation genes among the total number of genes adjacent to polymorphic LTRs is given in parentheses. Significant enrichments (FDR-adjusted P -values) are indicated in red. (B) Cluster dendrogram of wild strains calculated from the presence–absence of polymorphic Tf1 insertions. Approximately unbiased (AU) P -values are indicated for each node. Significant AUs are indicated in red.

phthalate. While this is not an exhaustive list, it supports the McClintock proposal that TEs reorganize the genome when cells are exposed to unfamiliar forms of stress, a condition she termed genome shock. The integration of Tf1 at a 1000 different promoters allows cells to fine-tune their individual stress responses in ways that are more likely to allow survival than relying on the existing broad network of the core stress response. An intriguing additional possibility is that through continued exposure to an unfamiliar stress, multiple insertions could accumulate in individual cells that together could form the foundation of a new gene regulatory network (GRN). These networks would be specific depending on the nature of the insult. The assembly of GRNs due to integration activity of TEs is a compelling model for how regulatory sequences of TEs have undergone widespread domestication in controlling GRNs (Feschotte 2008; Rebollo et al. 2012; Sundaram et al. 2014; Lynch et al. 2015; Chuong et al. 2016; Thompson et al. 2016). The network of LTRs associated with sporulation and other survival genes found in wild strains provides strong support that TE integration can create GRNs in natural populations.

YHL9632, and YHL9638 (Feng et al. 2013) along with the leu selectable plasmid pHL1288 by the lithium acetate transformation (Forsburg and Rhind 2006). Cells that allowed transformation were selected on media PM lacking leucine. The resulting colonies were then screened on media YES + G418 to identify cells that have lost their ability to grow on G418, indicating the presence of the AI within *neo*. The presence of the AI was confirmed by amplification of a 137-bp fragment between primers HL3510 and 3511.

The library of *S. pombe* containing genome-wide integration of Tf1-*neo* was constructed as previously described (Chatterjee et al. 2014) with the following modification: All incubations were carried out in PM media. Briefly, transposition was induced by expressing Tf1-*neo* from the plasmid pHL2944 in the diploid strain YHL5661, which lacked endogenous copies of Tf1. Transposition induced in media lacking vitamin B1 was then inhibited by addition of vitamin B1. The transposition frequency was monitored by transposition assay. When the transposition frequency reached 2%, cells containing a genomic Tf1-*neo* integration and lacking the plasmid pHL2944 were selected on YES media containing FOA and G418.

Methods

The lists of yeast strains, plasmids, and oligonucleotides used in this study are available in Supplemental Tables S3 through S5, respectively.

Media and growth of *S. pombe*

Rich media consisted of YES media (Forsburg and Rhind 2006). Minimal media consisted of PMG media supplemented with all amino acids (Forsburg and Rhind 2006). When indicated, vitamin B1 (Sigma) was added to a final concentration of 10 μ M to repress the promoter *mnt1*, 5-fluoroorotic acid (5-FOA; US Biologicals) to a final concentration of 1 mg/mL, and antibiotic Geneticin (G418; Gibco by Life Technologies) to a final concentration of 500 μ g/mL.

All *S. pombe* strains were grown at 32°C. The exposure to stress was carried out by supplementing the media as indicated: PMG liquid media were supplemented with CoCl₂ hexahydrate (Sigma) to a final concentration of 0.2 mM or 1.2 mM; PMG 2% agar Petri dishes were supplemented with CoCl₂ to a final concentration of 0.2 mM or 8 mM; caffeine (Sigma) 10 mM; ZnCl₂ (Sigma) 7.5 mM; or 50 mM potassium phthalate.

Yeast strains and plasmid construction

To monitor new transposition events occurring from the genomic copies of Tf1, an AI was introduced by homologous recombination within the sequence coding for the *neo*-resistance gene located within Tf1-*neo*. Briefly, strains containing Tf1 integrations 1, 2, 3, and 4 were obtained by introducing 5–10 μ g of a fragment containing the AI purified from the plasmid pHL692 into the Tf1-containing strains YHL9629, YHL9631,

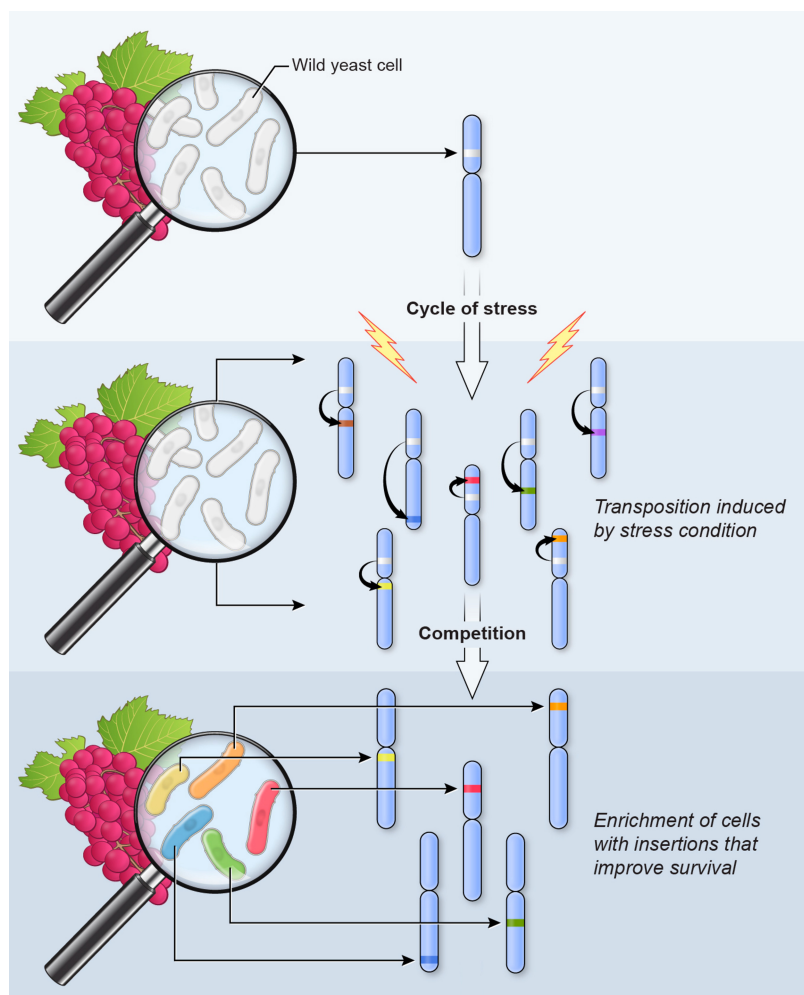


Figure 6. Model for adaptation through stress-induced mobilization of transposable elements. A single chromosome out of the three *S. pombe* chromosomes is represented to illustrate the mechanism. Repeated exposure to stress results in cycles of increased transposition. Insertions target different regions on any of the *S. pombe* chromosomes. Competition between cells containing new insertions results in the selection of sets of insertions that improve survival.

Strains containing deletions of nonessential genes were purchased from the Bioneer Company (library version 2; <http://pombe.bioneer.co.kr/>).

We reconstructed by homologous recombination the Tf1 integrations 5, 6, and 7, identified at Chr II position 3607268 (–), Chr I position 678437 (–), and Chr II position 3858489 (+), respectively. The diploid strain YHL5661 was transformed with 2–8 μ g of fragments containing the full-length Tf1-*neo* flanked by 80–500 bp of the target sequence, using the lithium acetate transformation. The fragment corresponding to Tf1 integrated at Chr II position 3858489 (+) was amplified with 80 bp of homology to the target site by fusion PCR using primers pairs HL3701-HL3702 and HL3703-HL3704 and then HL3710-HL3711. The amplification was performed using Expand long range dNTPack (Roche) according to the manufacturer’s recommendations. The fragments corresponding to the two other positions were commercially synthesized (<https://www.dna20.com/> for Chr II position 3607268 [–]; Life Technologies for Chr I 678437 [–]). Fragments contained a 500-bp homology to the target site, the 5’ sequence of Tf1 up to the AvrII restriction site, the 3’ sequence of Tf1 up to the XhoI restriction site, and another 500 bp homology to the target site.

The full-length Tf1 flanked by target homologies was then assembled by ligating the AvrII-XhoI fragment central section of Tf1 from pHL414 into the plasmids containing partial Tf1-*neo* flanked by sequences of the integration site (Supplemental Table S5). The resulting plasmids containing full Tf1-*neo* flanked by sequences of the integration site (Supplemental Table S5) were digested with 10 units of SpeI and used for lithium acetate transformation in order to achieve homologous recombination. Cells with Tf1 integrated at the loci of interest were selected onto YES containing G418. The presence of Tf1 at the expected integration site was confirmed by PCR amplification of a fragment spanning *neo* and the adjacent genomic region (primer pairs described in Supplemental Table S6) and by DNA blot (data not shown). The resulting yeast strains are described in Supplemental Table S4.

Transposition assay

Transposition frequency was calculated according to the protocol described previously (Chatterjee et al. 2014), with the following modifications to monitor new genomic integrations of Tf1. Cultures starting at OD=0.05 were incubated in 50 mL of PM media containing 0.2 mM CoCl₂, 7.5 mM ZnCl₂, 10 mM caffeine, or 50 mM phthalates. A solution of HCl was added at 8 mM to the media containing ZnCl₂ and the corresponding control media for ZnCl₂ solubility. Cultures were diluted to OD=5 and then diluted in a series of five 10-fold dilutions. The three lowest dilutions were spread onto YES plates, and the highest dilution, as well as a number of cells equivalent to 25 mL of culture, was spread on YES containing

G418. The AI allows the expression of the G418 resistance only in cells that have undergone a new genomic integration event (Levin 1995). After 3 d, the number of colonies were counted for three biological replicates, apart from integration 4 in 10 mM caffeine with only two biological replicates, and extrapolated to the number of cells in 1 mL of culture. The transposition frequency corresponds to the percentage of colonies resistant to G418. The number of generations achieved during the culture was determined by measuring the OD at the beginning and end of cultures. Transposition rates were calculated by dividing the transposition frequency by the number of generations. The *P*-values were calculated using Student’s *t*-test.

Competitive growth of the genome-wide library and determination of Tf1 integration profile

Triplicate 50-mL cultures were inoculated in PM with the library of *S. pombe* diploid cells YHL5661 containing Tf1-*neo* at an initial OD = 0.1. CoCl₂ was either omitted or added to a final concentration of 0.2 or 1.2 mM. The cultures were passaged for 80 generations. Each 24-h passage was diluted to OD=0.05 before adding CoCl₂.

Aliquots of 200 OD taken from the initial ($T=0$) and last ($T=80$) passage of each replicate cultures were spun down 5 min at 2187g, and the pellets were stored at -80°C . Genomic DNA was isolated and processed for Illumina sequencing of Tf1 integration sites according to the method of Chatterjee et al. (2014), with the following modifications: Genomic DNA was isolated using a MasterPure yeast DNA purification kit (Epicentre); four different barcodes located in sequencing custom primers HL3498, HL3512, HL3513, and HL3514 were coupled with the linker-specific primer HL2216 for multiplexing the Illumina sequencing reaction. The sequencing was performed on an HiSeq 2000 system at the University of California, Irvine Genomics High-Throughput Facility and the DNA Sequencing and Genomics Core of the National Heart, Lung, and Blood Institute.

Analysis of Tf1 integration profiles

The mapping of Tf1 integration sites to the *S. pombe* genome (unmasked EMBL release ASM294v2.21 from September 2009, ftp://ftp.ensemblgenomes.org/pub/fungi/release-21/fasta/schizosaccharomyces_pombe/dna/Schizosaccharomyces_pombe.ASM294v2.21.dna.genome.fa.gz) was performed using the custom scripts suite HTtools (Guo and Levin 2010; Supplemental Software S1). The relative proportion of cells containing a given Tf1 integration was extrapolated from the number of sequence reads and normalized to the total number of mapped sequence reads per replicate sample. An integration position was categorized as enriched when the number of sequence reads at this position and genomic orientation were increased by greater than two between the resulting culture ($T=80$) of each of the triplicate and the average of the starting culture ($T=0$). Only positions with five or greater sequence reads in the resulting cultures ($T=80$) were considered. Inversely, a position was categorized as depleted when the ratio was lower than 0.5 and had five or greater sequence reads in the initial cultures ($T=0$). To assess the statistical significance of intersections among the three sets of enriched positions in the 0.2 mM CoCl_2 cultures, we computed the probabilities of multiset intersections using SuperExactTest, an R package based on a density function of a hypergeometric model. The P -value for 106 enriched insertions overlapping in three replicates was $P < 1.47 \times 10^{-44}$ (Wang et al. 2015a).

Functional enrichment analysis

The 250 gene set analyzed was adjacent to positions enriched two-fold or more in three replicas grown in 0.2 mM of cobalt or was adjacent to positions enriched in at least one replicate in 1.2 mM of cobalt (Supplemental Table S1).

Functional enrichment analyses were performed against different sets of ontology annotations: *S. pombe* Process annotation (GO Term Finder; <http://go.princeton.edu/cgi-bin/GOTermFinder>), Fission Yeast Phenotype Ontology annotation (Harris et al. 2013), the set of genes up-regulated in *tor2* mutants (Matsuo et al. 2007), the set of genes up-regulated and down-regulated in *tor1Δ* strain (Schonbrun et al. 2009), and the set of genes induced by environmental stresses (Chen et al. 2003). Enrichments were calculated as the ratio of the proportion of ontology genes in the query relative to the proportion of the ontology genes among all RNA Pol II-transcribed genes (Supplemental Software S2). The P -values were calculated using the default setting of the GO Term Finder application for the Process annotation, using a hypergeometric test, and were corrected per gene set for false-discovery rates. As a control, we measured the length of intergenic regions with five or more insertions and found that regions flanking GO-annotated genes associated with enriched Tf1 integration

were not significantly larger than the ones flanking all genes used as background for the GO enrichment (Student's t -test followed by FDR adjustment).

Directional selection within intergenic regions was measured by averaging the Tajima's D based on the SNPs collection described previously (Jeffares et al. 2015). Tajima's D values were calculated using the option --TajimaD from VCFtools with a nonoverlapping sliding window of 200 bp (Danecek et al. 2011).

Drop assay

The resistance to CoCl_2 was determined by placing 10- μL drops of five consecutive fivefold dilutions of cells starting at $\text{OD}_{600}=0.5$ on PMG agar plates containing 0 or 8 mM of CoCl_2 . The plates were incubated for 4 d at 32°C .

Quantification of gene expression

Triplicate 5-mL cultures were inoculated in PM media at an initial $\text{OD}_{600}=0.01$. CoCl_2 was either omitted or added to a final concentrations as follows: For integrations 5 or 7, CoCl_2 was added at a concentration of 1.2 mM, and the cells were incubated for 24 h. For integration 6, cells were first incubated until they reached an $\text{OD}_{600}=1$, CoCl_2 was added at the concentration of 0.2 mM, and the cells were incubated an additional 1 h after addition of cobalt. For integrations 1, 2, 3, and 4, CoCl_2 was added at the concentration of 0.2 mM, and the cells were incubated for 24 h. Cells were then promptly spun down for 5 min at 2187g, and the pellets were stored at -80°C . Total RNA were isolated using the MasterPure yeast RNA purification kit (Epicentre). DNA traces were removed using TurboDNA-free (Ambion RNA by Life Technologies). Five hundred nanograms of RNAs were then reverse transcribed into cDNA using a high-capacity cDNA reverse-transcription kit (Applied Biosystems by Life Technologies). Gene expression was determined by quantitative PCR on a StepOnePlus system, with the following procedure: 6 μL cDNAs previously diluted to 10 ng/ μL , 10 μL of SYBR green PCR master mix (Applied Biosystems by Life Technologies), and 4 μL of forward and reverse primers mixed at 1 μM . The samples were analyzed in triplicate. Genes and Tf1 expressions were normalized to that of *act1* expression. Relative changes in expression were determined by the comparative C_T (ΔC_T) method (Schmittgen and Livak 2008). The P -values were calculated using Student's t -test.

Quantification of Tf1 transcription was carried out according to the same protocol with the following modifications: Cultures were inoculated in PM media at an initial $\text{OD}_{600}=0.05$ and incubated for 24 h at 32°C .

Data access

All raw data are publicly available. The DNA sequence data from this study have been submitted to the NCBI Sequence Read Archive (SRA; <https://www.ncbi.nlm.nih.gov/sra>) under accession number SRP142766. All custom codes used in this paper are available in Supplemental Software S1 and S2.

Acknowledgments

This research was supported by the Intramural Research Program of the National Institutes of Health (NIH) from the Eunice Kennedy Shriver National Institute of Child Health and Human Development.

Author contributions: C.E. and H.L.L. contributed to study design and manuscript preparation. C.E., M.L., and C.H. contributed to experimental results.

References

- Atwood A, Choi J, Levin HL. 1998. The application of a homologous recombination assay revealed amino acid residues in an LTR-retrotransposon that were critical for integration. *J Virol* **72**: 1324–1333.
- Bourque G, Leong B, Vega VB, Chen X, Lee YL, Srinivasan KG, Chew JL, Ruan Y, Wei CL, Ng HH, et al. 2008. Evolution of the mammalian transcription factor binding repertoire via transposable elements. *Genome Res* **18**: 1752–1762. doi:10.1101/gr.080663.108
- Cairns J, Foster PL. 1991. Adaptive reversion of a frameshift mutation in *Escherichia coli*. *Genetics* **128**: 695–701.
- Cairns J, Overbaugh J, Miller S. 1988. The origin of mutants. *Nature* **335**: 142–145. doi:10.1038/335142a0
- Chantranupong L, Wolfson RL, Sabatini DM. 2015. Nutrient-sensing mechanisms across evolution. *Cell* **161**: 67–83. doi:10.1016/j.cell.2015.02.041
- Chantranupong L, Scaria SM, Saxton RA, Gygi MP, Shen K, Wyant GA, Wang T, Harper JW, Gygi SP, Sabatini DM. 2016. The CASTOR proteins are arginine sensors for the mTORC1 pathway. *Cell* **165**: 153–164. doi:10.1016/j.cell.2016.02.035
- Chatterjee AG, Esnault C, Guo Y, Hung S, McQueen PG, Levin HL. 2014. Serial number tagging reveals a prominent sequence preference of retrotransposon integration. *Nucleic Acids Res* **42**: 8449–8460. doi:10.1093/nar/gku534
- Chen DR, Toone WM, Mata J, Lyne R, Burns G, Kivinen K, Brazma A, Jones N, Bahler J. 2003. Global transcriptional responses of fission yeast to environmental stress. *Mol Biol Cell* **14**: 214–229. doi:10.1091/mbc.e02-08-0499
- Chénais B, Caruso A, Hiard S, Casse N. 2012. The impact of transposable elements on eukaryotic genomes: from genome size increase to genetic adaptation to stressful environments. *Gene* **509**: 7–15. doi:10.1016/j.gene.2012.07.042
- Chuong EB, Elde NC, Feschotte C. 2016. Regulatory evolution of innate immunity through co-option of endogenous retroviruses. *Science* **351**: 1083–1087. doi:10.1126/science.aad5497
- Curcio MJ, Lutz S, Lesage P. 2015. The Ty1 LTR-retrotransposon of budding yeast, *Saccharomyces cerevisiae*. *Microbiol Spectr* **3**: MDNA3-0053-2014. doi:10.1128/microbiolspec.MDNA3-0053-2014
- Dainty SJ, Kennedy CA, Watt S, Bähler J, Whitehall SK. 2008. Response of *Schizosaccharomyces pombe* to zinc deficiency. *Eukaryot Cell* **7**: 454–464. doi:10.1128/EC.00408-07
- Danecek P, Auton A, Abecasis G, Albers CA, Banks E, DePristo MA, Handsaker RE, Lunter G, Marth GT, Sherry ST, et al. 2011. The variant call format and VCFtools. *Bioinformatics* **27**: 2156–2158. doi:10.1093/bioinformatics/btr330
- Eickbush TH, Eickbush DG. 2015. Integration, regulation, and long-term stability of R2 retrotransposons. *Microbiol Spectr* **3**: MDNA3-0011-2014. doi:10.1128/microbiolspec.MDNA3-0011-2014
- Eltshinger S, Loewith R. 2016. TOR complexes and the maintenance of cellular homeostasis. *Trends Cell Biol* **26**: 148–159. doi:10.1016/j.tcb.2015.10.003
- Esnault C, Levin HL. 2015. The long terminal repeat retrotransposons Tf1 and Tf2 of *Schizosaccharomyces pombe*. *Microbiol Spectr* **3**: MDNA3-0040-2014. doi:10.1128/microbiolspec.MDNA3-0040-2014
- Faulkner GJ, Kimura Y, Daub CO, Wani S, Plessy C, Irvine KM, Schroder K, Cloonan N, Steptoe AL, Lassmann T, et al. 2009. The regulated retrotransposon transcriptome of mammalian cells. *Nat Genet* **41**: 563–571. doi:10.1038/ng.368
- Feng G, Leem YE, Levin HL. 2013. Transposon integration enhances expression of stress response genes. *Nucleic Acids Res* **41**: 775–789. doi:10.1093/nar/gks1185
- Feschotte C. 2008. Transposable elements and the evolution of regulatory networks. *Nat Rev Genet* **9**: 397–405. doi:10.1038/nrg2337
- Forsburg SL, Rhind N. 2006. Basic methods for fission yeast. *Yeast* **23**: 173–183. doi:10.1002/yea.1347
- Gallo S, Gatti S, Sala V, Albano R, Costelli P, Casanova E, Comoglio PM, Crepaldi T. 2014. Agonist antibodies activating the Met receptor protect cardiomyoblasts from cobalt chloride-induced apoptosis and autophagy. *Cell Death Dis* **5**: e1185. doi:10.1038/cddis.2014.155
- Goberdhan DC, Wilson C, Harris AL. 2016. Amino acid sensing by mTORC1: Intracellular transporters mark the spot. *Cell Metab* **23**: 580–589. doi:10.1016/j.cmet.2016.03.013
- Guo Y, Levin HL. 2010. High-throughput sequencing of retrotransposon integration provides a saturated profile of target activity in *Schizosaccharomyces pombe*. *Genome Res* **20**: 239–248. doi:10.1101/gr.099648.109
- Harris MA, Lock A, Bahler J, Oliver SG, Wood V. 2013. FYPO: the fission yeast phenotype ontology. *Bioinformatics* **29**: 1671–1678. doi:10.1093/bioinformatics/btt266
- Hashida SN, Kitamura K, Mikami T, Kishima Y. 2003. Temperature shift coordinately changes the activity and the methylation state of transposon Tam3 in *Antirrhinum majus*. *Plant Physiol* **132**: 1207–1216. doi:10.1104/pp.102.017533
- Hashida SN, Uchiyama T, Martin C, Kishima Y, Sano Y, Mikami T. 2006. The temperature-dependent change in methylation of the *Antirrhinum* transposon Tam3 is controlled by the activity of its transposase. *Plant Cell* **18**: 104–118. doi:10.1105/tpc.105.037655
- Hickey A, Esnault C, Majumdar A, Chatterjee AG, Iben JR, McQueen PG, Yang AX, Mizuguchi T, Grewal SI, Levin HL. 2015. Single-nucleotide-specific targeting of the Tf1 retrotransposon promoted by the DNA-binding protein Sap1 of *Schizosaccharomyces pombe*. *Genetics* **201**: 905–924. doi:10.1534/genetics.115.181602
- Horvath V, Merenciano M, Gonzalez J. 2017. Revisiting the relationship between transposable elements and the eukaryotic stress response. *Trends Genet* **33**: 832–841. doi:10.1016/j.tig.2017.08.007
- Jacobs JZ, Rosado-Lugo JD, Cranz-Mileva S, Ciccaglione KM, Tournier V, Zaratiegui M. 2015. Arrested replication forks guide retrotransposon integration. *Science* **349**: 1549–1553. doi:10.1126/science.aaa3810
- Jardim SS, Schuch AP, Pereira CM, Loreto EL. 2015. Effects of heat and UV radiation on the mobilization of transposon *mariner-Mos1*. *Cell Stress Chaperones* **20**: 843–851. doi:10.1007/s12192-015-0611-2
- Jeffares DC, Rallis C, Rieux A, Speed D, Prevorsevsky M, Mourier T, Marsellach FX, Iqbal Z, Lau W, Cheng TM, et al. 2015. The genomic and phenotypic diversity of *Schizosaccharomyces pombe*. *Nat Genet* **47**: 235–241. doi:10.1038/ng.3215
- Jordan IK, Rogozin IB, Glazko GV, Koonin EV. 2003. Origin of a substantial fraction of human regulatory sequences from transposable elements. *Trends Genet* **19**: 68–72. doi:10.1016/S0168-9525(02)00006-9
- Lee H, Bien CM, Hughes AL, Espenshade PJ, Kwon-Chung KJ, Chang YC. 2007. Cobalt chloride, a hypoxia-mimicking agent, targets sterol synthesis in the pathogenic fungus *Cryptococcus neoformans*. *Mol Microbiol* **65**: 1018–1033. doi:10.1111/j.1365-2958.2007.05844.x
- Leem YE, Ripmaster TL, Kelly FD, Ebina H, Heincelman ME, Zhang K, Grewal SI, Hoffman CS, Levin HL. 2008. Retrotransposon Tf1 is targeted to Pol II promoters by transcription activators. *Molecular Cell* **30**: 98–107. doi:10.1016/j.molcel.2008.02.016
- Levin HL. 1995. A novel mechanism of self-primed reverse transcription defines a new family of retroelements. *Mol Cell Biol* **15**: 3310–3317. doi:10.1128/MCB.15.6.3310
- Levin HL, Moran JV. 2011. Dynamic interactions between transposable elements and their hosts. *Nat Rev Genet* **12**: 615–627. doi:10.1038/nrg3030
- Loewith R, Hall MN. 2011. Target of rapamycin (TOR) in nutrient signaling and growth control. *Genetics* **189**: 1177–1201. doi:10.1534/genetics.111.133363
- Lynch VJ, Nnamani MC, Kapusta A, Brayer K, Plaza SL, Mazur EC, Emera D, Sheikh SZ, Grutzner F, Bauersachs S, et al. 2015. Ancient transposable elements transformed the uterine regulatory landscape and transcriptome during the evolution of mammalian pregnancy. *Cell Rep* **10**: 551–561. doi:10.1016/j.celrep.2014.12.052
- Macfarlan TS, Gifford WD, Driscoll S, Lettieri K, Rowe HM, Bonanomi D, Firth A, Singer O, Trono D, Pfaff SL. 2012. Embryonic stem cell potency fluctuates with endogenous retrovirus activity. *Nature* **487**: 57–63. doi:10.1038/nature11244
- Mahat DB, Salamanca HH, Duarte FM, Danko CG, Lis JT. 2016. Mammalian heat shock response and mechanisms underlying its genome-wide transcriptional regulation. *Mol Cell* **62**: 63–78. doi:10.1016/j.molcel.2016.02.025
- Maisnier-Patin S, Roth JR. 2015. The origin of mutants under selection: how natural selection mimics mutagenesis (adaptive mutation). *Cold Spring Harb Perspect Biol* **7**: a018176. doi:10.1101/cshperspect.a018176
- Majumdar S, Rio DC. 2015. P transposable elements in *Drosophila* and other eukaryotic organisms. *Microbiol Spectr* **3**: MDNA3-0004-2014. doi:10.1128/microbiolspec.MDNA3-0004-2014
- Matsuo T, Otsubo Y, Urano J, Tamanoi F, Yamamoto M. 2007. Loss of the TOR kinase Tor2 mimics nitrogen starvation and activates the sexual development pathway in fission yeast. *Mol Cell Biol* **27**: 3154–3164. doi:10.1128/MCB.01039-06
- McClintock B. 1984. The significance of responses of the genome to challenge. *Science* **226**: 792–801. doi:10.1126/science.15739260
- Mele M, Ferreira PG, Reverter F, DeLuca DS, Monlong J, Sammeth M, Young TR, Goldmann JM, Pervouchine DD, Sullivan TJ, et al. 2015. Human genomics: the human transcriptome across tissues and individuals. *Science* **348**: 660–665. doi:10.1126/science.aaa0355
- Miousse IR, Chalbot MC, Lumen A, Ferguson A, Kavouras IG, Koturbash I. 2015. Response of transposable elements to environmental stressors. *Mutat Res Rev Mutat Res* **765**: 19–39. doi:10.1016/j.mrrrev.2015.05.003
- Morales ME, Servant G, Ade C, Roy-Engel AM. 2015. Altering genomic integrity: Heavy metal exposure promotes transposable element-mediated damage. *Biol Trace Elem Res* **166**: 24–33. doi:10.1007/s12011-015-0298-3

- Morimoto RI. 1998. Regulation of the heat shock transcriptional response: cross talk between a family of heat shock factors, molecular chaperones, and negative regulators. *Genes Dev* **12**: 3788–3796. doi:10.1101/gad.12.24.3788
- Rai SK, Sangesland M, Lee M Jr, Esnault C, Cui Y, Chatterjee AG, Levin HL. 2017. Host factors that promote retrotransposon integration are similar in distantly related eukaryotes. *PLoS Genet* **13**: e1006775. doi:10.1371/journal.pgen.1006775
- Rebollo R, Romanish MT, Mager DL. 2012. Transposable elements: an abundant and natural source of regulatory sequences for host genes. *Annu Rev Genet* **46**: 21–42. doi:10.1146/annurev-genet-110711-155621
- Rebsamen M, Pochini L, Stasyk T, de Araujo ME, Galluccio M, Kandasamy RK, Snijder B, Fauster A, Rudashevskaya EL, Bruckner M, et al. 2015. SLC38A9 is a component of the lysosomal amino acid sensing machinery that controls mTORC1. *Nature* **519**: 477–481. doi:10.1038/nature14107
- Rosenthal GA. 1977. The biological effects and mode of action of L-canavanine, a structural analogue of L-arginine. *Q Rev Biol* **52**: 155–178. doi:10.1086/409853
- Roth JR, Kugelberg E, Reams AB, Kofoid E, Andersson DI. 2006. Origin of mutations under selection: the adaptive mutation controversy. *Annu Rev Microbiol* **60**: 477–501. doi:10.1146/annurev.micro.60.080805.142045
- Sandmeyer S, Patterson K, Bilanchone V. 2015. Ty3, a position-specific retrotransposon in budding yeast. *Microbiol Spectr* **3**: MDNA3-0057-2014. doi:10.1128/microbiolspec.MDNA3-0057-2014
- Saxton RA, Chantranupong L, Knockenhauer KE, Schwartz TU, Sabatini DM. 2016. Mechanism of arginine sensing by CASTOR1 upstream of mTORC1. *Nature* **536**: 229–233. doi:10.1038/nature19079
- Schmittgen TD, Livak KJ. 2008. Analyzing real-time PCR data by the comparative C_T method. *Nat Protoc* **3**: 1101–1108. doi:10.1038/nprot.2008.73
- Schonbrun M, Laor D, Lopez-Maury L, Bahler J, Kupiec M, Weisman R. 2009. TOR complex 2 controls gene silencing, telomere length maintenance, and survival under DNA-damaging conditions. *Mol Cell Biol* **29**: 4584–4594. doi:10.1128/MCB.01879-08
- Sehgal A, Lee CY, Espenshade PJ. 2007. SREBP controls oxygen-dependent mobilization of retrotransposons in fission yeast. *PLoS Genet* **3**: e131. doi:10.1371/journal.pgen.0030131
- Simonsen LO, Harbak H, Bennekou P. 2012. Cobalt metabolism and toxicology: a brief update. *Sci Total Environ* **432**: 210–215. doi:10.1016/j.scitotenv.2012.06.009
- Sultana T, Zamborlini A, Cristofari G, Lesage P. 2017. Integration site selection by retroviruses and transposable elements in eukaryotes. *Nat Rev Genet* **18**: 292–308. doi:10.1038/nrg.2017.7
- Sundaram V, Cheng Y, Ma Z, Li D, Xing X, Edge P, Snyder MP, Wang T. 2014. Widespread contribution of transposable elements to the innovation of gene regulatory networks. *Genome Res* **24**: 1963–1976. doi:10.1101/gr.168872.113
- Tajima F. 1989. Statistical method for testing the neutral mutation hypothesis by DNA polymorphism. *Genetics* **123**: 585–595.
- Tan VP, Miyamoto S. 2016. Nutrient-sensing mTORC1: integration of metabolic and autophagic signals. *J Mol Cell Cardiol* **95**: 31–41. doi:10.1016/j.yjmcc.2016.01.005
- Thompson PJ, Macfarlan TS, Lorincz MC. 2016. Long terminal repeats: from parasitic elements to building blocks of the transcriptional regulatory repertoire. *Mol Cell* **62**: 766–776. doi:10.1016/j.molcel.2016.03.029
- Todeschini AL, Morillon A, Springer M, Lesage P. 2005. Severe adenine starvation activates Ty1 transcription and retrotransposition in *Saccharomyces cerevisiae*. *Mol Cell Biol* **25**: 7459–7472. doi:10.1128/MCB.25.17.7459-7472.2005
- Vihervaara A, Duarte FM, Lis JT. 2018. Molecular mechanisms driving transcriptional stress responses. *Nat Rev Genet* doi:10.1038/s41576-018-0001-6
- Wang M, Zhao Y, Zhang B. 2015a. Efficient test and visualization of multi-set intersections. *Sci Rep* **5**: 16923. doi:10.1038/srep16923
- Wang T, Birsoy K, Hughes NW, Krupczak KM, Post Y, Wei JJ, Lander ES, Sabatini DM. 2015b. Identification and characterization of essential genes in the human genome. *Science* **350**: 1096–1101. doi:10.1126/science.aac7041
- Weisman R. 2016. Target of rapamycin (TOR) regulates growth in response to nutritional signals. *Microbiol Spectr* **4**: FUNK-0006-2016. doi:10.1128/microbiolspec.FUNK-0006-2016
- Workman JJ, Chen H, Larabee RN. 2014. Environmental signaling through the mechanistic target of rapamycin complex 1: mTORC1 goes nuclear. *Cell Cycle* **13**: 714–725. doi:10.4161/cc.28112
- Yamayoshi I, Maisnier-Patin S, Roth JR. 2018. Selection-enhanced mutagenesis of *lac* genes is due to their coamplification with *dinB* encoding an error-prone DNA polymerase. *Genetics* **208**: 1009–1021. doi:10.1534/genetics.117.300409
- Yang T, Li D, Liu F, Qi L, Yan G, Wang M. 2015. Regulation on Beclin-1 expression by mTOR in CoCl₂-induced HT22 cell ischemia-reperfusion injury. *Brain Res* **1614**: 60–66. doi:10.1016/j.brainres.2015.04.016
- Zhong X, Lin R, Li Z, Mao J, Chen L. 2014. Effects of *Salidroside* on cobalt chloride-induced hypoxia damage and mTOR signaling repression in PC12 cells. *Biol Pharm Bull* **37**: 1199–1206. doi:10.1248/bpb.b14-00100
- Zhong R, Xu H, Chen G, Zhao G, Gao Y, Liu X, Ma S, Dong L. 2015. The role of hypoxia-inducible factor-1 α in radiation-induced autophagic cell death in breast cancer cells. *Tumour Biol* **36**: 7077–7083. doi:10.1007/s13277-015-3425-z

Received May 17, 2018; accepted in revised form November 15, 2018.